Circadian rhythm shows potential for mRNA efficiency and self-organized division of labor in multinucleate cells

Leif Zinn-Brooks[1*], Marcus L. Roper[2†]

1 Department of Mathematics, Harvey Mudd College, Claremont, California, USA
2 Department of Mathematics, UCLA, Los Angeles, California, USA

* lzinnbrooks@hmc.edu
† mroper@math.ucla.edu

Abstract

Multinucleate cells occur in every biosphere and across the kingdoms of life, including in the human body as muscle cells and bone-forming cells. Data from filamentous fungi suggest that, even when bathed in a common cytoplasm, nuclei are capable of autonomous behaviors, including division. How does this potential for autonomy affect the organization of cellular processes between nuclei? Here we analyze a simplified model of circadian rhythm, a form of cellular oscillator, in a mathematical model of the filamentous fungus *Neurospora crassa*. Our results highlight the role played by mRNA-protein phase separation to keep mRNAs close to the nuclei from which they originate, while allowing proteins to diffuse freely between nuclei. Our modeling shows that syncytism allows for extreme mRNA efficiency — we demonstrate assembly of a robust oscillator with transcription levels 10^4-fold less than in comparable uninucleate cells. We also show self-organized division of the labor of mRNA production, with one nucleus in a two-nucleus syncytium producing at least twice as many mRNAs as the other in 30% of cycles. This division can occur spontaneously, but division of labor can also be controlled by regulating the amount of cytoplasmic volume available to each nucleus. Taken together, our results show the intriguing richness and potential for emergent organization among nuclei in multinucleate cells. They also highlight the role of previously studied mechanisms of cellular organization, including nuclear space control and localization of mRNAs through RNA-protein phase separation, in regulating nuclear coordination.

Author summary

Circadian rhythms are among the most researched cellular processes, but limited work has been done on how these rhythms are coordinated between nuclei in multinucleate cells. In this work, we analyze a mathematical model for circadian oscillations in a multinucleate cell, motivated by frequency mRNA and protein data from the filamentous fungus *Neurospora crassa*. Our results illuminate the importance of mRNA-protein phase separation, in which mRNAs are kept close to the nucleus in which they were transcribed, while proteins can diffuse freely across the cell. We demonstrate that this phase separation allows for a robust oscillator to be assembled with very low mRNA counts. We also investigate how the labor of transcribing mRNAs is divided between nuclei, both when nuclei are evenly spaced across the cell and when they are not. Division of this labor can be regulated by controlling the amount of

cytoplasmic volume available to each nucleus. Our results show that there is potential for emergent organization and extreme mRNA efficiency in multinucleate cells.

Introduction

Syncytia, or multinucleate cells, are present throughout the human body, as muscle cells and bone forming cells, as well as in embryos [1–3]. They also occur in every biosphere and across the kingdoms of life, including fungi, slime molds, and water molds [4–7]. Yet, despite their ubiquity in nature, we do not know how closely cellular processes within syncytia, such as nuclear division, growth, or secretion of enzymes, resemble or diverge from processes in uninucleate cells [8]. In particular, unlike a uninucleate cell, there are many possible ways for a syncytium to divide the labor of making mRNAs among its nuclei. Can syncytial nuclei coordinate the transcription of mRNAs to divide labor among themselves?

The genetics of circadian rhythms are among the most throughly dissected of cellular processes [9], and we will use them as a paradigm for how labor of producing mRNAs may be divided between nuclei. The rhythms are fundamental to the life of the cell, regulating timing of the cell cycle and sleep-wake cycle, while also influencing cell physiology, metabolism, and behavior [10–13]. Circadian clocks can be entrained by external cues such as light and temperature, but are also capable of persisting in the absence of these cues [14]. Many circadian rhythms are characterized by biochemical oscillations (such as fluctuations in mRNA and protein concentrations) with period ~ 24 h, and circadian clocks are typically regulated by transcription-translation feedback loops [14–16].

The filamentous fungus *Neurospora crassa* alternates between growth during the day and spore production at night [16, 17]. Circadian timekeeping is regulated by the clock gene *frq* (frequency) and its interactions with WCC (White Collar Complex). Interlocking positive and negative feedback loops drive oscillations of the *frq* gene: in the positive feedback loop, WCC enters the nucleus and activates *frq* transcription. *frq* mRNA is then translated to FRQ protein, which promotes the accumulation of WC-1 and WC-2, the proteins that comprise the White Collar Complex. In the negative feedback loop, FRQ promotes phosphorylation of WCC, which inactivates the complex, thereby preventing it from activating *frq* transcription [13, 18].

Ordinary differential equation models have shown that the known interactions between FRQ and WCC mRNAs and proteins are sufficient to drive *Neurospora's* circadian rhythm. Tseng et al. [18] developed a comprehensive model of the *Neurospora* circadian clock, including every key clock component. The authors showed that their model is capable of reproducing a wide variety of clock characteristics, including a consistent period length, maintained in constant light conditions, and entrainment to photoperiods. They then isolated the crucial components that influence the period and amplitude of oscillations. Dovzhenok et al. [13] formulated a simpler model to study glucose compensation of the *Neurospora* circadian clock, and also to investigate the effect of molecular noise on the robustness of FRQ protein oscillations.

These models are capable of producing qualitatively correct time-varying amounts of FRQ and WCC proteins. However, recent data, in which single molecule Fluorescence In-Situ Hybridization (smFISH) was used to map distribution of *frq* mRNAs, indicate that the mRNAs that drive the circadian rhythm are at far lower densities than can support oscillations in the existing ODE models. Remarkably, these data show that at peak transcription, there may be only 6 copies of mRNA per nucleus (Brad Bartholomai, personal communication, 2019). Moreover, low abundance mRNAs are likely to be strongly affected by Poisson noise; do fluctuations in mRNA density affect the precision of the clock?

Prior modeling of Neurospora's circadian rhythm has also omitted the syncytial context, treating the fungal nuclei as a single compartment and the cytoplasm as a second compartment [13, 18, 19]. The models are therefore silent on how the elements of the oscillator are assembled across tens, hundreds, or possibly even thousands of nuclei. Indeed, competing hypotheses can be advanced: averaging mRNA and protein abundances in many nuclei may reduce the effect of fluctuations, or, if different oscillators interfere, it may lead to less tightly controlled oscillations.

Although models directly addressing *Neurospora's* circadian rhythm qualitatively capture its clock components, there are too many unmeasured parameters in these models to use them to make quantitative predictions. For this reason, we analyze the syncytial version of a simpler rhythm, which uses a single negative feedback loop to time its clock. In using this model, we limit ourselves to making only semi-quantitative predictions about the real clock. Nonetheless, our model resolves the interplay of Poisson noise, the need to synchronize multiple nuclei, and differential sharing of mRNAs and proteins between nuclei based on their different mobilities within the cytoplasm.

Our syncytial cell model is adapted from Wang and Peskin's [20] single cell model for the mammalian circadian rhythm, which is based on the abundance of PER (PERIOD) proteins. In this model, a single negative feedback loop maintains the clock, driving circadian oscillation of PER mRNA and protein levels. The circadian oscillation manifests as a limit cycle, which is attained only above a critical rate of mRNA transcription. Wang and Peskin [20] considered the destabilizing effect of Poisson noise on this limit cycle, as well as showing how the model can be modified to incorporate entrainment by light. In this work, we ask whether stable oscillations can be achieved with lower mRNA costs in a syncytial organism. Along the way, our model signals the existence of a potential general benefit to syncytial organization by allowing predictable protein abundances to emerge from mRNAs with low and fluctuation-affected transcription rates because of the pooling of proteins between nuclei. Mathematically, we must go beyond existing models, which incorporate only temporally varying protein and mRNA concentrations, to model the distribution of mRNAs and proteins within the cell. Our model operates in a regime dominated by the effects of Poisson noise, with mRNA copy numbers, matched to experiments, one or two orders of magnitude smaller than those in previous models.

We begin by describing our mathematical model for circadian rhythms in a syncytial cell. We then run stochastic simulations of our model (using the Gillespie algorithm [21]) for a single nuclear compartment with transcription rates several orders of magnitude below the parameter value used by Wang and Peskin [20], matching the mRNA abundances seen in real fungal cells. We show that stochastic transcription can maintain quasi-periodic limit cycles for transcription rates far below the deterministic threshold at which Wang and Peskin [20] first see limit cycles emerging. We develop a quantitative measure for evaluating the quality of model circadian limit cycles, and measure this "quality factor" for a range of transcription rates. Subsequently, we turn to a syncytial context, and show that protein diffusion between nuclear compartments regulates circadian rhythms in a syncytium by demonstrating that limit cycles are more "organized" (i.e., have a higher quality factor) in a model syncytium than in a uninucleate cell with the same mRNA and protein expression levels. Finally, we demonstrate that protein diffusion also has an "entrainment" effect on our model syncytial cell by comparing protein oscillations in linked nuclear compartments to oscillations in autonomous nuclei.

1 Mathematical Model

How is the circadian clock coordinated between nuclei in a multinucleate cell such as *Neurospora*? To address this question, we adapt for syncytial cells the single negative feedback model formulated by Wang and Peskin [20], which was originally proposed for the mammalian circadian oscillator. Our model represents a simplified form of the timing machinery in real *Neurospora* cells since it incorporates only a negative feedback loop, so our predictions will be semi-quantitative at best. Nonetheless, our model allows us to incorporate the elements that are most important for this analysis: stochastic fluctuations and very small mRNA copy numbers.

Our model syncytium is a line of length L, divided into N compartments of equal length (in Section 2.3.2, we will consider non-uniform compartment lengths). Each compartment (index $i = 1, 2, ..., N$) consists of a nucleus (n) at its center and a surrounding cytoplasm (c), with volumes V_n and V_c, respectively. There are four state variables, mRNA M and protein P, each present in the nucleus and cytoplasm. Only proteins within the boundaries of a compartment (i.e., in the local cytoplasm) can be imported into that compartment's nucleus. Our notation is

$$\begin{aligned} M_n^{(i)} &= \text{concentration of nuclear mRNA in compartment } i, \\ M_c^{(i)} &= \text{concentration of cytoplasmic mRNA in compartment } i, \\ P_c^{(i)} &= \text{concentration of cytoplasmic protein in compartment } i, \\ P_n^{(i)} &= \text{concentration of nuclear protein in compartment } i. \end{aligned}$$

Nuclear mRNAs are transcribed at maximum rate α; this transcription is inhibited by nuclear protein. Nuclear mRNAs are also exported out of the nucleus and into their local cytoplasm (at rate γ_m), where they translate protein (at rate β) and decay (at rate δ_m). We assume that diffusion of cytoplasmic mRNAs is limited due to their relatively large molecular size [22], and potentially is further reduced by specific interactions between mRNAs and proteins that confine mRNAs within high viscosity droplets in the cell [23]. Hence, cytoplasmic mRNAs remain in the compartment containing the nucleus from which they originated. Within each compartment, our ODEs for M_n and M_c are the same as in [20]:

$$\frac{dM_n^{(i)}}{dt} = \underbrace{\frac{\alpha}{V_n}\left(\frac{K}{K + P_n^{(i)}}\right)^r}_{\text{transcription}} - \underbrace{\gamma_m M_n^{(i)}}_{\text{export}}, \tag{1}$$

$$\frac{dM_c^{(i)}}{dt} = \underbrace{\gamma_m \left(\frac{V_n}{V_c}\right) M_n^{(i)}}_{\text{export}} - \underbrace{\delta_m M_c^{(i)}}_{\text{decay}}. \tag{2}$$

For the derivation of the term for nuclear mRNA transcription, see [20].

Cytoplasmic proteins are imported into their local nucleus (at rate γ_p), where they decay (at rate δ_p). The ODE for cytoplasmic protein in each compartment is

$$\frac{dP_c^{(i)}}{dt} = \underbrace{\beta M_c^{(i)}}_{\text{translation}} - \underbrace{\gamma_p P_c^{(i)}}_{\text{import}}. \tag{3}$$

In contrast to nuclear mRNAs, however, cytoplasmic proteins can also move between compartments via diffusion. We make the simplifying assumption that diffusion of proteins is "fast" relative to the rates of protein translation and import (for details on

this assumption and its implications for our model, see the Appendix). Hence, following either one of these reactions, the distribution of cytoplasmic proteins in our syncytium instantaneously reaches equilibrium (i.e., a uniform concentration of proteins across the entire cell). This is achieved by averaging the concentration of cytoplasmic proteins across all compartments, and then assigning this average concentration to each compartment:

$$P_c^{(i)} := \frac{1}{N}\sum_{i=1}^{N} P_c^{(i)}. \tag{4}$$

In our stochastic simulations, we impose that whenever the total number of proteins P_{tot} in the cytoplasm changes (via translation or import into the nucleus), the proteins are redistributed so that each compartment contains $\lfloor P_{\text{tot}}/N \rfloor$ proteins, with the remaining proteins (if any) randomly assigned to separate compartments. We use the same equation as [20] for protein in each nucleus:

$$\frac{dP_n^{(i)}}{dt} = \underbrace{\gamma_p \left(\frac{V_c}{V_n}\right) P_c^{(i)}}_{\text{import}} - \underbrace{\delta_p P_n^{(i)}}_{\text{decay}}. \tag{5}$$

2 Results

2.1 Stochastic transcription maintains limit cycles below the threshold for deterministic oscillations

Wang and Peskin [20] showed that their deterministic model produces sustained (rather than damped) oscillations only above a critical peak rate of transcription:

$$\alpha > 4 \cdot 5^5 \cdot \nu^2 \cdot \frac{KV_n}{\beta}, \tag{6}$$

where, for simplicity, γ_m, γ_p, δ_m, δ_p are all set equal to ν. With the default parameter values used by [20] ($\nu = 2\pi/22\ h^{-1}$, $V_n = 0.1$ pL, $\beta = 10\ h^{-1}$, $K = 200$/pL), (6) predicts that a limit cycle will be maintained for $\alpha > 2039\ h^{-1}$. While the authors ran many stochastic simulations using their default transcription rate ($\alpha = 180000\ h^{-1}$), they did not explore the behavior of the stochastic model when α is below the deterministic threshold for a limit cycle. Using the Gillespie algorithm [21], we ran trials of the Wang and Peskin [20] model (i.e., our mathematical model with $N = 1$ compartment) for values of α three and four orders of magnitude below the default rate ($\alpha = 180\ h^{-1}$ and $\alpha = 18\ h^{-1}$, respectively). Note that both of these rates are in a regime where the deterministic model displays damped oscillations. Interestingly, while oscillations of protein and mRNA levels in the deterministic model rapidly decay, oscillations are maintained indefinitely in the stochastic model (Fig 1).

Fig 1. Stochastic transcription preserves limit cycles.
Deterministic (thick blue curve) vs. stochastic (thin red curve) time course for nuclear protein for $\alpha = 18\ h^{-1}$ (A) and $\alpha = 180\ h^{-1}$ (B). In (A) and (B), α values are two and one orders of magnitude, respectively, below the critical transcription rate derived from (6), so under the deterministic model, oscillations are damped. However, stochastic realizations of the same model support sustained, albeit noisy, oscillations.

In Fig 2, we display time course data from a single stochastic simulation for $\alpha = 18\ h^{-1}$, the lowest transcription rate we tested, and for $\alpha = 180000\ h^{-1}$, the default parameter value used by Wang and Peskin [20]. On average, we find that mRNA counts

are about an order of magnitude higher for $\alpha = 180000\ h^{-1}$, and that counts for $\alpha = 18\ h^{-1}$ are much closer to experimental data from *Neurospora*. Remarkably, periodic oscillations are still evident in the $\alpha = 18\ h^{-1}$ case, even with peak mRNA counts in the single digits.

Fig 2. mRNA oscillations are still evident even at a very low transcription rate.
Time course of number of mRNA copies in the nucleus from individual stochastic simulations using two extremal values of the transcription rate α.

2.2 Measuring the quality of limit cycles

To compare different conditions, we develop a quantitative measure of the the "quality" of limit cycles in the stochastic circadian rhythm model. To begin, we find the power spectrum for P_n over 1000 h of simulated time, averaged over $N = 100$ trials. The power spectrum of a time series gives the power of each frequency component in the signal, computed using Fourier analysis [24]. The peak in the power spectrum indicates the dominant frequency of the signal; a noisy signal that does not have a limit cycle will have a peak of zero. A reliable circadian oscillator should have a consistent period; accordingly, we define the "quality factor" q of our oscillator to be the proportion of the total power that is within a certain time τ of the peak period T^*, i.e.,

$$q = \frac{\int_{\omega_-}^{\omega_+} P(\omega)d\omega}{\int_0^{\infty} P(\omega)d\omega},$$

where P = power, ω = frequency, and

$$\omega_- = \frac{1}{T^* + \tau}, \quad \omega_+ = \frac{1}{T^* - \tau}.$$

For all subsequent measures of quality factor, we use $\tau = 2\ h$. In Fig 3, we show examples of evaluating quality factor for $\alpha = 18\ h^{-1}$ and $\alpha = 180000\ h^{-1}$.

Fig 3. Power spectrum can be used to measure the periodicity of the circadian rhythm.
We average the power spectrum for nuclear protein over 100 trials, with a low transcription rate (A) and a high transcription rate (B). The quality factor is the fraction of the power spectrum in the interval $[\omega_-, \omega_+]$ (shaded areas) to the total area under the curve. Red asterisks indicate the peak frequency. Quality factors are $q = 0.192$ in (A) and $q = 0.370$ in (B).

We compute the quality factor for five orders of magnitude of the transcription rate α, ranging from $\alpha = 18\ h^{-1}$ to $\alpha = 180000\ h^{-1}$. We find that quality factor increases with α (see Table 1) since mRNA and protein counts are generally higher for larger values of α, making oscillations of nuclear protein less susceptible to Poisson noise. So, although we predict that circadian oscillations can be maintained even when transcription rate is low, oscillations will be more regular in amplitude and period when transcription rate is high. However, gains are modest: quality factor q increases only by a factor of 2 for a 10^4-fold increase in α.

Table 1. Maximum transcription rate α vs. quality factor q of nuclear protein oscillations.

α (h^{-1})	Quality factor (q)
18	0.192
180	0.227
1800	0.251
18000	0.304
180000	0.370

2.3 Limit cycle quality in a model syncytium

2.3.1 Uniform compartment sizes

We now evaluate the quality factor of nuclear protein oscillations for multiple nuclear compartments ($N = 2$, 4, 8, and 16 compartments) of equal length (i.e., each nucleus contains the same volume of surrounding cytoplasm). As before, we find the power spectrum for 1000 h of simulated time, averaged over 100 trials. Since we expect quality factor to be consistent across compartments, and we would like to compare with the one compartment case, we evaluate the quality factor for a single compartment in each case, rather than for the entire cell. We find that quality factor increases with number of compartments in the syncytium (Fig 4). This is likely because the redistribution of cytoplasmic proteins has an averaging effect on the model, removing some of the noise. As the number of compartments increases, this averaging effect becomes more robust. In fact, the quality factor with 8 or 16 nuclear compartments at the lowest transcription rate is comparable to the quality factor for a single compartment at the highest transcription rate.

Fig 4. Quality factor increases with transcription rate and number of compartments.
Quality factor for 1, 2, 4, 8, and 16 nuclear compartments, over five orders of magnitude of the maximum transcription rate α.

Sharing transcription-inhibiting proteins evenly between nuclear compartments of uniform size results in roughly equal average transcription rates in each nucleus, leading to an improvement of limit cycle quality. But how is the labor of transcribing mRNAs divided between nuclei over each circadian day? To investigate, we ran a stochastic simulation of our model for a model syncytium with two compartments of equal length and with the minimal transcription rate $\alpha = 18\ h^{-1}$, and counted the number of mRNAs transcribed in each compartment over each circadian period. (We define a circadian period as the time interval between troughs in nuclear protein expression.) The simulation was run for 10000 h (approximately 400 periods). We find that the labor of producing mRNAs often skews strongly toward a single compartment over individual periods (Fig 5). In fact, in nearly 30% of periods, one nucleus produces more than twice the number of mRNAs as the other.

Fig 5. mRNA production in a model syncytium with uniform compartments.
(A) Number of mRNAs transcribed in each nuclear compartment for approximately 400 circadian periods for a two-nucleus syncytium with uniform compartment sizes (1:1 size ratio). The red line represents equal numbers of mRNAs being produced by each nucleus. (B) Histogram of the results from (A) indicates that one compartment often dominates mRNA production over a single period.

Asymmetries in mRNA production apparently emerge spontaneously from the circadian dynamics. Controlling division of labor may confer selective benefits upon fungi. The feedback strength depends on the number of proteins a nucleus encounters, and thus depends on the volume of cytoplasm in that nucleus' compartment. What happens to circadian cycles when these cytoplasmic volumes are not equal (i.e., nuclear compartments are not of uniform size)? We address this question in the next section.

2.3.2 Non-uniform compartment sizes

In general, nuclear compartment sizes are not exactly uniform in a syncytial cell (though in some syncytial cells, cytoskeletal elements closely regulate internuclear spacing [25]). Because proteins are uniformly distributed in the cytoplasm in our model, the expected number of cytoplasmic proteins in compartment i at time t is

$$E[P_c^{(i)}(t)] = \frac{l_i}{\sum_{i=1}^{N} l_i} P_{\text{tot}}(t), \tag{7}$$

where l_i is the length of compartment i. In *Neurospora*, nuclear movement and rearrangement constantly modify compartment sizes [26]. For simplicity, we assume that compartment sizes remain constant over time: our model is designed to identify trends in how labor is divided between nuclei, rather than to quantitatively model the real *Neurospora* circadian clock. By examining Eqs (1) and (5), we can infer the effect of compartment size on mRNA transcription. Since larger compartments generally contain more cytoplasmic proteins than smaller ones, it follows that more proteins are imported into nuclei contained within larger compartments. Thus, transcription rates are inhibited more in larger compartments, meaning that mRNA levels should decrease as compartment size increases. To verify this hypothesis, we ran simulations of a two compartment syncytium in which the larger compartment is double the length of the smaller. We find that the smaller compartment contains dramatically more mRNAs than the larger, in both the nucleus and surrounding cytoplasm (Fig 6). Hence, labor of transcription is unevenly divided between compartments, and nuclei in small compartments carry much more of the burden of producing mRNAs.

Fig 6. Nuclei in smaller compartments do more labor of producing mRNAs.
mRNA time courses for nucleus (left panel) and cytoplasm (right panel) from a stochastic simulation of a two-nucleus syncytium in which one compartment is twice the length of the other, for $\alpha = 180\ h^{-1}$.

To further study division of labor for unequal compartment sizes, we repeated the simulation from section 2.3.1, this time for a variety of two-compartment model syncytia, in which the larger compartment was $1.1, 1.2, ..., 1.5$ times the length of the smaller compartment. As before, simulations were run for 10000 h, with transcription rate $\alpha = 18\ h^{-1}$. In Fig 7, we display scatter plots for the 1.1x and 1.5x cases. We focus specifically on the skew in the number of transcribed mRNAs — i.e., the fraction of mRNAs that are transcribed by the nucleus in the smaller compartment. Although we find that mRNA product is unevenly distributed between nuclei from cycle to cycle, uneven compartment sizes consistently bias mRNA production from cycle to cycle. Mean mRNA production skews slightly towards the smaller compartment in the 1.1x case, and dramatically towards the smaller compartment in the 1.5x case (data on mean transcription fractions shown for all cases in Table 2).

Is limit cycle quality substantially reduced when mRNA production asymmetries are induced by changing compartment sizes? To answer this question, we ran 100

Fig 7. Compartment size differences skew the relative number of mRNAs transcribed by each nucleus.
Number of mRNAs transcribed in each nuclear compartment for approximately 400 circadian periods in two different two-nucleus syncytia (panel titles indicate size ratios). The red line represents equal numbers of mRNAs being produced by each nucleus.

Table 2. Ratio of compartment lengths l_1/l_2 vs. fraction of total mRNAs transcribed in compartment 2 (the smaller compartment).

l_1/l_2	mean fraction transcribed in comp. 2
1.1	0.559
1.2	0.600
1.3	0.654
1.4	0.688
1.5	0.731

realizations of our stochastic model for each of the two-compartment model syncytia outlined above; each realization was run for 1000 h. Since quality factor varies with compartment size, we compute the quality factor for the entire cell in each case (i.e. we find the quality factor for the *total* number of nuclear proteins) rather than for a single compartment. We then compare this set of quality factors to the factor for an entire cell composed of two compartments of equal length. We find that increasing variability in compartment length has a very minimal effect of limit cycle quality (Fig 8). Our results show that even with extreme division of labor between nuclei, a high quality oscillator can be assembled. The nucleus in the larger compartment, though it produces the minority of the cell's mRNAs, contributes enough to ensure that the quality factor remains consistently larger than the factor for a uninucleate cell (0.192 for the parameter values assayed here).

Fig 8. Quality factor (across the entire cell) is close to uniform for a variety of two-nucleus syncytia.
We varied the asymmetry of compartment sizes and measured the mean quality of the oscillator over 1000 simulated hours, with $\alpha = 18\ h^{-1}$. Quality factor varies little and consistently exceeds the value for a uninucleate cell (0.192).

2.3.3 Limit cycle consistency in a model syncytium

Lastly, we wish to examine whether protein sharing supports consistency of circadian timekeeping in a model syncytium when transcription rate is very low ($\alpha = 18\ h^{-1}$). We return to uniform compartment sizes, as in Section 2.3.1, and consider two different scenarios: (i) eight nuclear compartments that share proteins via diffusion and (ii) eight autonomous nuclear compartments, with each compartment containing only the mRNAs and proteins produced by its nucleus. In both scenarios, every compartment is given the same initial conditions, i.e.,

$$M_n^{(1)}(0) = M_n^{(2)}(0) = ... = M_n^{(8)}(0) = \mu_n, \quad M_c^{(1)}(0) = M_c^{(2)}(0) = ... = M_c^{(8)}(0) = \mu_c,$$
$$P_c^{(1)}(0) = P_c^{(2)}(0) = ... = P_c^{(8)}(0) = \rho_c, \quad P_n^{(1)}(0) = P_n^{(2)}(0) = ... = P_n^{(8)}(0) = \rho_n,$$

where μ_n, μ_c, ρ_c, and ρ_n are constants. Starting from these initial conditions, we simulate five circadian "days" for the two different scenarios outlined above. In this context, a "day" refers to the time period between peaks in total nuclear protein expression (i.e., the total nuclear protein count for the entire cell). We are interested in

evaluating the consistency in the timing of these peaks. We therefore ran 100 stochastic simulations for each scenario, with the same initial conditions for every trial, and recorded the time that each peak occurred for each simulation.

In Fig 9, we display histograms for the times that peaks occurred, where time 0 h indicates the time for the first peak. Unsurprisingly, we find that the timing of peaks becomes more unpredictable over time. However, since the nuclei from scenario (i) share proteins, oscillations for nuclear protein in each compartment are roughly in-phase from their initially synchronized states. On the other hand, in scenario (ii), nuclei have no means to "communicate," so nuclear protein oscillations drift quickly out of phase. Hence, timing of peaks in *total* nuclear protein is considerably more unpredictable in scenario (ii) than in scenario (i), as indicated by larger standard deviations for peak times in scenario (ii) (Fig 9). This shows that protein diffusion can help regulate circadian timekeeping in a syncytial cell, and that circadian rhythms quickly break down in a syncytial cell with no communication between its nuclei. In the absence of external cues such as light, circadian rhythms tend to deteriorate after several days [16, 27]. However, we've shown that, like light, protein sharing between nuclei can have an entraining (synchronizing) effect on the cell's rhythms, helping maintain reliable rhythms for a longer period of time.

Fig 9. Protein sharing supports a consistent circadian rhythm.
Times of peaks of total nuclear protein expression, for eight nuclear compartments that share proteins (A) and eight autonomous nuclear compartments (B). We ran 100 simulations in each case, with $\alpha = 18\ h^{-1}$. In each figure, we also indicate the standard deviation σ_i of peak time for each circadian "day" ($i = 1, 2, ..., 5$). Expected times for peaks (i.e., average circadian day lengths) are indicated with blue diamonds.

Discussion

We have formulated and simulated a mathematical model for circadian rhythms in a syncytial cell, adapted from the uninucleate model of Wang and Peskin [20]. The motivation for developing our model was to better understand division of labor (i.e., partitioning of mRNA transcription) between nuclei in *Neurospora crassa*. Our results indicate that, by "sharing" proteins between nuclei via molecular diffusion, nuclei within a syncytial cell such as *Neurospora* can achieve a robust, reliable circadian rhythm with minimal mRNA production. For example, we found that a model syncytium with eight nuclei can achieve nuclear protein oscillations of comparable "quality" to a uninucleate cell while reducing transcription rates by a factor of ten thousand (see Section 2.3.1). This is because protein sharing has an averaging effect on the model, removing much of the consequences of random mRNA fluctuations. While our model is undoubtedly simplified, it offers a potential explanation of recent experimental results, which suggest that *Neurospora* achieves a robust circadian rhythm with very small mRNA counts (Brad Bartholomai, personal communication, 2019).

Many of the simulations in this paper were run below the deterministic threshold for a Hopf bifurcation derived in [20] (see the inequality (6)). We selected this regime of the model because we wanted to test whether oscillations could be achieved at the very low transcription rates that are consistent with smFISH measurements of mRNA in *Neurospora crassa* (Brad Bartholomai, personal communication, 2019). Remarkably, we found that, even in uninucleate systems, quasi-periodic limit cycles are attained in stochastic simulations when the transcription rate is two orders of magnitude lower than this threshold and mRNA counts are in the single digits. However, absolute quantification of proteins is very difficult in syncytial cells [28], so the actual translation

rates in *Neurospora* may be considerably higher than the parameter value we used. A high translation rate β could potentially push the system back into the regime where a deterministic limit cycle exists. Regardless, it is notable that random transcription events can potentially maintain limit cycles for very low transcription rates, allowing a cell to achieve a robust circadian rhythm with minimal labor upon its nuclei.

Extreme mRNA efficiency may confer fitness advantages upon fungal cells. These cells are often regarded as enzyme factories — capable of expressing vast quantities of potentially useful proteins [29]. Although the energetic cost of mRNA transcription is not large, the physical rearrangements needed to access a particular gene may create interference when a nucleus must access multiple different regions of its genome to express multiple genes [30]. Reducing transcription rates on each gene may therefore allow a nucleus to transcribe a larger set of genes. In Zaslaver et al. [30], the authors highlight that organisms may benefit from minimizing the rates of transcription, while keeping protein abundances constant. The super-secretory abilities and rapid growth of fungi may emerge from their ability to push transcription rates to extremely low rates while using protein sharing to suppress stochastic fluctuations in the abundances of the proteins produced.

In constructing our syncytial cell model, we made the simplifying assumption that protein diffusion is "fast" relative to protein import and decay. Hence, we imposed that protein levels are constantly uniformized between compartments. While this assumption may be fairly reasonable across a small number of nuclear compartments, it breaks down for a larger cell with many nuclear compartments. So, while our model predicts that limit cycle quality increases with number of nuclei (Fig. 4), is there a trade-off that occurs in a larger cell, as communication between nuclei becomes more limited? A model that includes more accurate diffusive mechanics could help answer this question, and better predict how spacing of nuclei across the cell affects the quality of circadian rhythms.

In future, it may be valuable to adapt our syncytial model to more closely describe circadian rhythms in *Neurospora*. FRQ mRNA and protein oscillations in *Neurospora* are driven by interlocking positive and negative feedback loops, while our model involves only a negative feedback loop. A minimal differential equation model to study *Neurospora* circadian rhythm would likely need to include FRQ mRNA and protein, White Collar mRNA and protein, and FRQ-White Collar complex (whose formation inhibits *frq* transcription). A model including all of these elements could potentially allow quantitative matching to the emerging data streams on real mRNA and protein abundances [31, 32].

Appendix

High diffusivity of protein justifies treating protein concentrations as uniform

In Section 2 we stated that, since diffusion of cytoplasmic proteins is "fast" relative to the rates of protein translation and import, we can reasonably ignore diffusive mechanics, and simply assume that cytoplasmic protein concentration is at all times uniform across the syncytium. This assumption allows us to greatly reduce the number of time steps in numerical simulations. Below is a justification for this assumption.

We begin by rewriting our syncytial circadian rhythm model, but with diffusion between nuclear compartments included. Suppose that cytoplasmic proteins move into adjacent compartments at rate ξ, with reflecting boundary conditions at each end of the cell. We use the same parameter values for import, export, and decay as in [20], and set them equal to each other: $\gamma_m = \delta_m = \gamma_p = \delta_p = \nu$. The model equations read as follows:

$$\frac{dM_n^{(i)}}{dt} = \frac{\alpha}{V_n}\left(\frac{K}{K+P_n^{(i)}}\right)^r - \nu M_n^{(i)}, \quad i = 1, ..., N; \tag{8}$$

$$\frac{dM_c^{(i)}}{dt} = \nu\left(\frac{V_n}{V_c}\right)M_n^{(i)} - \nu M_c^{(i)}, \quad i = 1, ..., N; \tag{9}$$

$$\frac{dP_c^{(i)}}{dt} = \beta M_c^{(i)} - \nu P_c^{(i)} + \xi\left(P_c^{(i-1)} - 2P_c^{(i)} + P_c^{(i+1)}\right), \quad i = 2, ..., N-1, \tag{10}$$

$$\frac{dP_c^{(1)}}{dt} = \beta M_c^{(1)} - \nu P_c^{(1)} + \xi(P_c^{(2)} - P_c^{(1)}),$$

$$\frac{dP_c^{(N)}}{dt} = \beta M_c^{(N)} - \nu P_c^{(N)} + \xi(P_c^{(N-1)} - P_c^{(N)});$$

$$\frac{dP_n^{(i)}}{dt} = \nu\left(\frac{V_c}{V_n}\right)P_c^{(i)} - \nu P_n^{(i)}, \quad i = 1, ..., N. \tag{11}$$

Let $m_n = V_n M_n$, $m_c = V_c M_c$, $p_c = V_c P_c$, and $p_n = V_n P_n$. Also, let $\tau = \nu t$, $\tilde{\alpha} = \alpha/\nu$, and $\kappa = V_n K$. Then we have

$$\frac{dm_n^{(i)}}{d\tau} = \tilde{\alpha}\left(\frac{\kappa}{\kappa+p_n^{(i)}}\right)^r - m_n^{(i)}, \quad i = 1, ..., N; \tag{12}$$

$$\frac{dm_c^{(i)}}{d\tau} = m_n^{(i)} - m_c^{(i)}, \quad i = 1, ..., N; \tag{13}$$

$$\frac{dp_c^{(i)}}{d\tau} = \frac{\beta}{\nu}m_c^{(i)} - p_c^{(i)} + \frac{\xi}{\nu}\left(p_c^{(i-1)} - 2p_c^{(i)} + p_c^{(i+1)}\right), \quad i = 2, ..., N-1, \tag{14}$$

$$\frac{dp_c^{(1)}}{d\tau} = \frac{\beta}{\nu}m_c^{(1)} - p_c^{(1)} + \frac{\xi}{\nu}(p_c^{(2)} - p_c^{(1)}),$$

$$\frac{dp_c^{(N)}}{d\tau} = \frac{\beta}{\nu}m_c^{(N)} - p_c^{(N)} + \frac{\xi}{\nu}(p_c^{(N-1)} - p_c^{(N)});$$

$$\frac{dp_n^{(i)}}{d\tau} = p_c^{(i)} - p_n^{(i)}, \quad i = 1, ..., N. \tag{15}$$

Now, let's estimate the rate parameter ξ. Let D be the diffusion coefficient for cytoplasmic protein and l be the length of each nuclear compartment. To reach an adjacent compartment, each protein must travel a distance of $l/2$, on average. From [33], the mean time $\overline{T}$ for a protein to be displaced by $l/2$ is

$$\overline{T} = \frac{1}{2D}\left(\frac{l}{2}\right)^2 = \frac{l^2}{8D}.$$

It follows that the average rate of exchange of proteins between compartments is

$$\xi = \frac{1}{\overline{T}} = \frac{8D}{l^2}.$$

The diffusivity of a protein depends on its size and the viscosity of the cytosol through which the protein diffuses; for example, (small) GFP proteins have a diffusion coefficient of approximately 33 $\mu m^2/s$ in the cells of the filamentous fungus *Aspergillus niger* [34]. However, the molecular mass of FRQ protein (108 kDa) is 4 times greater than that of GFP (27 kDA), so, assuming a globular structure, we would expect its diffusivity to be

reduced by a factor of $4^{1/3}$ [33], which gives $D \approx 21\ \mu\text{m}^2/s$. Now, assuming that $l = 5$ μm, we obtain

$$\xi \approx 6.7\ s^{-1} \approx 24000\ h^{-1}.$$

Since we use $\nu = 2\pi/22 \approx 0.3\ h^{-1}$, $\epsilon := \nu/\xi$ is a very small dimensionless parameter. Multiplying both sides of Eq (14) by ϵ, we obtain the following dimensionless system:

$$\frac{dm_n^{(i)}}{d\tau} = \tilde{\alpha}\left(\frac{\kappa}{\kappa + p_n^{(i)}}\right)^r - m_n^{(i)}, \quad i = 1, ..., N; \tag{16}$$

$$\frac{dm_c^{(i)}}{d\tau} = m_n^{(i)} - m_c^{(i)}, \quad i = 1, ..., N; \tag{17}$$

$$\epsilon\frac{dp_c^{(i)}}{d\tau} = \epsilon\left(\tilde{\beta}m_c^{(i)} - p_c^{(i)}\right) + \left(p_c^{(i-1)} - 2p_c^{(i)} + p_c^{(i+1)}\right), \quad i = 2, ..., N-1, \tag{18}$$

$$\epsilon\frac{dp_c^{(1)}}{d\tau} = \epsilon\left(\tilde{\beta}m_c^{(1)} - p_c^{(1)}\right) + (p_c^{(2)} - p_c^{(1)}),$$

$$\epsilon\frac{dp_c^{(N)}}{d\tau} = \epsilon\left(\tilde{\beta}m_c^{(N)} - p_c^{(N)}\right) + (p_c^{(N-1)} - p_c^{(N)});$$

$$\frac{dp_n^{(i)}}{d\tau} = p_c^{(i)} - p_n^{(i)}, \quad i = 1, ..., N, \tag{19}$$

where $\tilde{\beta} = \beta/\nu$. Now, setting ϵ to 0 gives the "fast" dynamics for cytoplasmic protein:

$$p_c^{(i-1)} - 2p_c^{(i)} + p_c^{(i+1)} = 0 \quad (i = 2, ..., N-1); \quad p_c^{(1)} = p_c^{(2)}, \quad p_c^{(N)} = p_c^{(N-1)}.$$

Solving this system and returning to the original variables gives

$$P_c^{(1)} = P_c^{(2)} = ... = P_c^{(N)},$$

i.e., a uniform concentration of proteins across the cytoplasm of the cell. The "slow" dynamics for cytoplasmic protein are obtained by collecting $\mathcal{O}(\epsilon)$ terms in Eq (14):

$$\frac{dp_c^{(i)}}{d\tau} = \tilde{\beta}m_c^{(i)} - p_c^{(i)}.$$

In terms of the original parameters and variables,

$$\frac{dP_c^{(i)}}{dt} = \underbrace{\beta M_c^{(i)}}_{\text{translation}} - \underbrace{\gamma_p P_c^{(i)}}_{\text{import}}.$$

This analysis supports our assumption that protein concentrations are kept continuously uniform between compartments.

Acknowledgments

MR acknowledges financial support from the National Science Foundation under grant MCB-1840273.

References

1. Braun T, Gautel M. Transcriptional mechanisms regulating skeletal muscle differentiation, growth and homeostasis. Nat Rev Mol Cell Bio. 2011;12(6):349–361.

2. Cowin S. Mechanosensation and fluid transport in living bone. J Musculoskel Neuron. 2002;2(3):256–260.

3. Mavrakis M, Rikhy R, Lippincott-Schwartz J. Plasma Membrane Polarity and Compartmentalization are Established Before Cellularization in the Fly Embryo. Dev Cell. 2009;16(1):93–104.

4. Roper M, Ellison C, Taylor JW, Glass NL. Nuclear and genome dynamics in multinucleate ascomycete fungi. Curr Biol. 2011;21(18):R786–R793.

5. Roper M, Lee C, Hickey PC, Gladfelter AS. Life as a moving fluid: fate of cytoplasmic macromolecules in dynamic fungal syncytia. Curr Opin Microbiol. 2015;26:116–122.

6. Jockusch BM, Brown DF, Rusch HP. Synthesis and some properties of an actin-like nuclear protein in the slime mold *Physarum polycephalum*. J Bacteriol. 1971;108(2):705–714.

7. Rollins-Smith LA, Woodhams DC. Amphibian immunity. Oxford University Press New York; 2012.

8. Roberts SE, Gladfelter AS. Nuclear autonomy in multinucleate fungi. Curr Opin Microbiol. 2015;28:60–65.

9. Wager-Smith K, Kay SA. Circadian rhythm genetics: from flies to mice to humans. Nat Genet. 2000;26(1):23–27.

10. Hunt T, Sassone-Corsi P. Riding tandem: circadian clocks and the cell cycle. Cell. 2007;129(3):461–464.

11. Harrisingh MC, Nitabach MN. Integrating circadian timekeeping with cellular physiology. Science. 2008;320(5878):879–880.

12. Peschel N, Chen KF, Szabo G, Stanewsky R. Light-dependent interactions between the *Drosophila* circadian clock factors cryptochrome, jetlag, and timeless. Curr Biol. 2009;19(3):241–247.

13. Dovzhenok AA, Baek M, Lim S, Hong CI. Mathematical modeling and validation of glucose compensation of the *Neurospora* circadian clock. Biophys J. 2015;108(7):1830–1839.

14. Dunlap JC, Loros JJ. Making time: conservation of biological clocks from fungi to animals. In: The Fungal Kingdom. Wiley Online Library; 2017. p. 515–534.

15. Dunlap JC. Molecular bases for circadian clocks. Cell. 1999;96(2):271–290.

16. Dunlap J, Loros J, Colot H, Mehra A, Belden W, Shi M, et al. A circadian clock in Neurospora: how genes and proteins cooperate to produce a sustained, entrainable, and compensated biological oscillator with a period of about a day. In: Cold Spring Harbor Symposia on Quantitative Biology. vol. 72. Cold Spring Harbor Laboratory Press; 2007. p. 57–68.

17. Kramer C. Rhythmic conidiation in Neurospora crassa. In: Circadian Rhythms. Springer; 2007. p. 49–65.

18. Tseng YY, Hunt SM, Heintzen C, Crosthwaite SK, Schwartz JM. Comprehensive modelling of the Neurospora circadian clock and its temperature compensation. PLoS Comput Biol. 2012;8(3):e1002437.

19. François P. A Model for the *Neurospora* Circadian Clock. Biophys J. 2005;88(4):2369–2383.

20. Wang G, Peskin CS. Entrainment of a cellular circadian oscillator by light in the presence of molecular noise. Phys Rev E. 2018;97(6):062416.

21. Gillespie DT. Exact stochastic simulation of coupled chemical reactions. J Phys Chem-US. 1977;81(25):2340–2361.

22. Milo R, Phillips R. Cell Biology by the Numbers. Garland Science; 2015.

23. Dundon SE, Chang SS, Kumar A, Occhipinti P, Shroff H, Roper M, et al. Clustered nuclei maintain autonomy and nucleocytoplasmic ratio control in a syncytium. Mol Biol Cell. 2016;27(13):2000–2007.

24. Stoica P, Moses RL, et al. Spectral Analysis of Signals. Pearson Prentice Hall Upper Saddle River, NJ; 2005.

25. Anderson CA, Eser U, Korndorf T, Borsuk ME, Skotheim JM, Gladfelter AS. Nuclear repulsion enables division autonomy in a single cytoplasm. Curr Biol. 2013;23(20):1999–2010.

26. Roper M, Simonin A, Hickey PC, Leeder A, Glass NL. Nuclear dynamics in a fungal chimera. P Natl Acad Sci USA. 2013;110(32):12875–12880.

27. Baker CL, Loros JJ, Dunlap JC. The circadian clock of *Neurospora crassa*. FEMS Microbiology Rev. 2012;36(1):95–110.

28. Kirkpatrick DS, Gerber SA, Gygi SP. The absolute quantification strategy: a general procedure for the quantification of proteins and post-translational modifications. Methods. 2005;35(3):265–273.

29. Reilly MC, Qin L, Craig JP, Starr TL, Glass NL. Deletion of homologs of the SREBP pathway results in hyper-production of cellulases in Neurospora crassa and Trichoderma reesei. Biotechnol Biofuels. 2015;8(1):121.

30. Zaslaver A, Kaplan S, Bren A, Jinich A, Mayo A, Dekel E, et al. Invariant distribution of promoter activities in *Escherichia coli*. PLoS Comput Biol. 2009;5(10):e1000545.

31. Hong CI, Zámborszky J, Baek M, Labiscsak L, Ju K, Lee H, et al. Circadian rhythms synchronize mitosis in Neurospora crassa. P Natl Acad Sci USA. 2014;111(4):1397–1402.

32. Caster SZ, Castillo K, Sachs MS, Bell-Pedersen D. Circadian clock regulation of mRNA translation through eukaryotic elongation factor eEF-2. P Natl Acad Sci USA. 2016;113(34):9605–9610.

33. Nelson P. Biological Physics. WH Freeman New York; 2004.

34. Bleichrodt RJ, Hulsman M, Wösten HA, Reinders MJ. Switching from a unicellular to multicellular organization in an *Aspergillus niger* hypha. mBio. 2015;6(2).

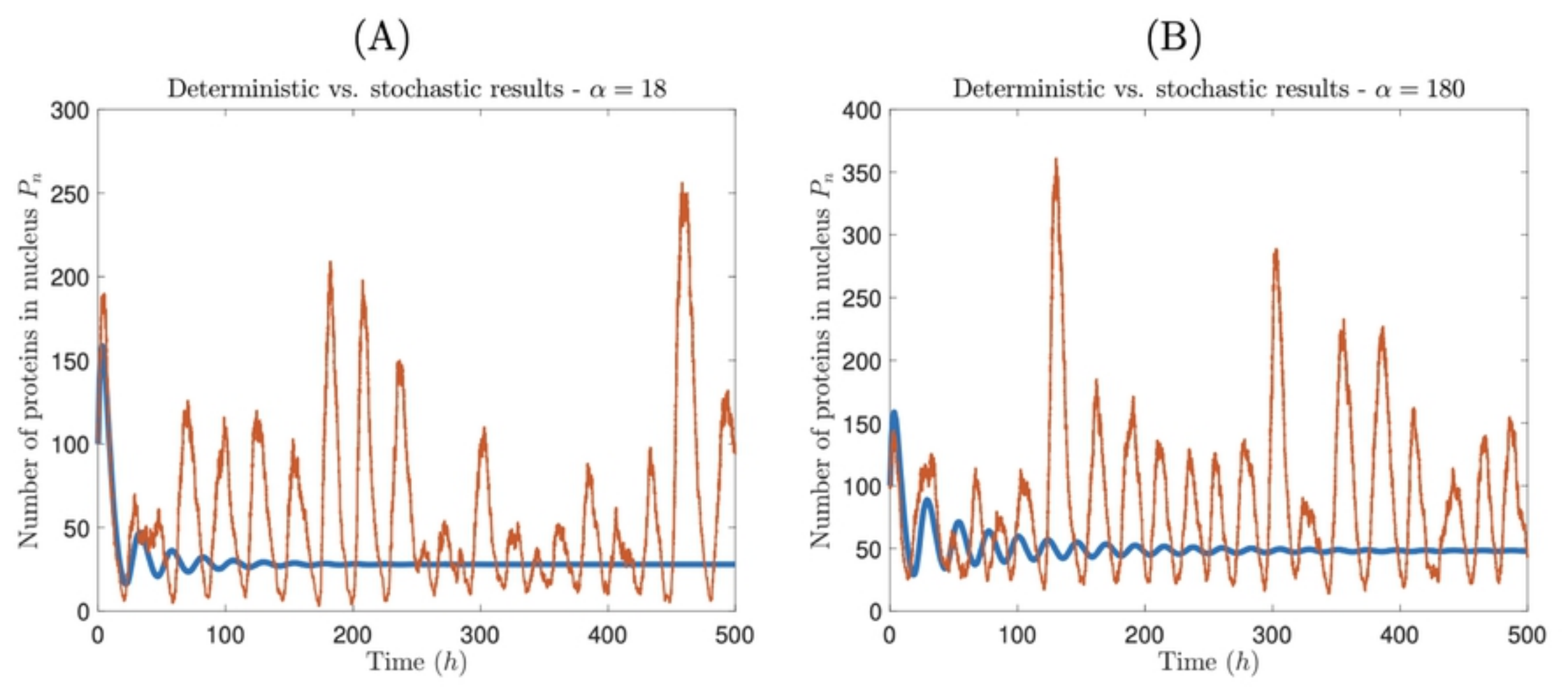
(A)
Deterministic vs. stochastic results - $\alpha = 18$
Number of proteins in nucleus P_n
Time (h)
0
50
100
150
200
250
300
0
100
200
300
400
500
(B)
Deterministic vs. stochastic results - $\alpha = 180$
Number of proteins in nucleus P_n
Time (h)
0
50
100
150
200
250
300
350
400
0
100
200
300
400
500

Figure

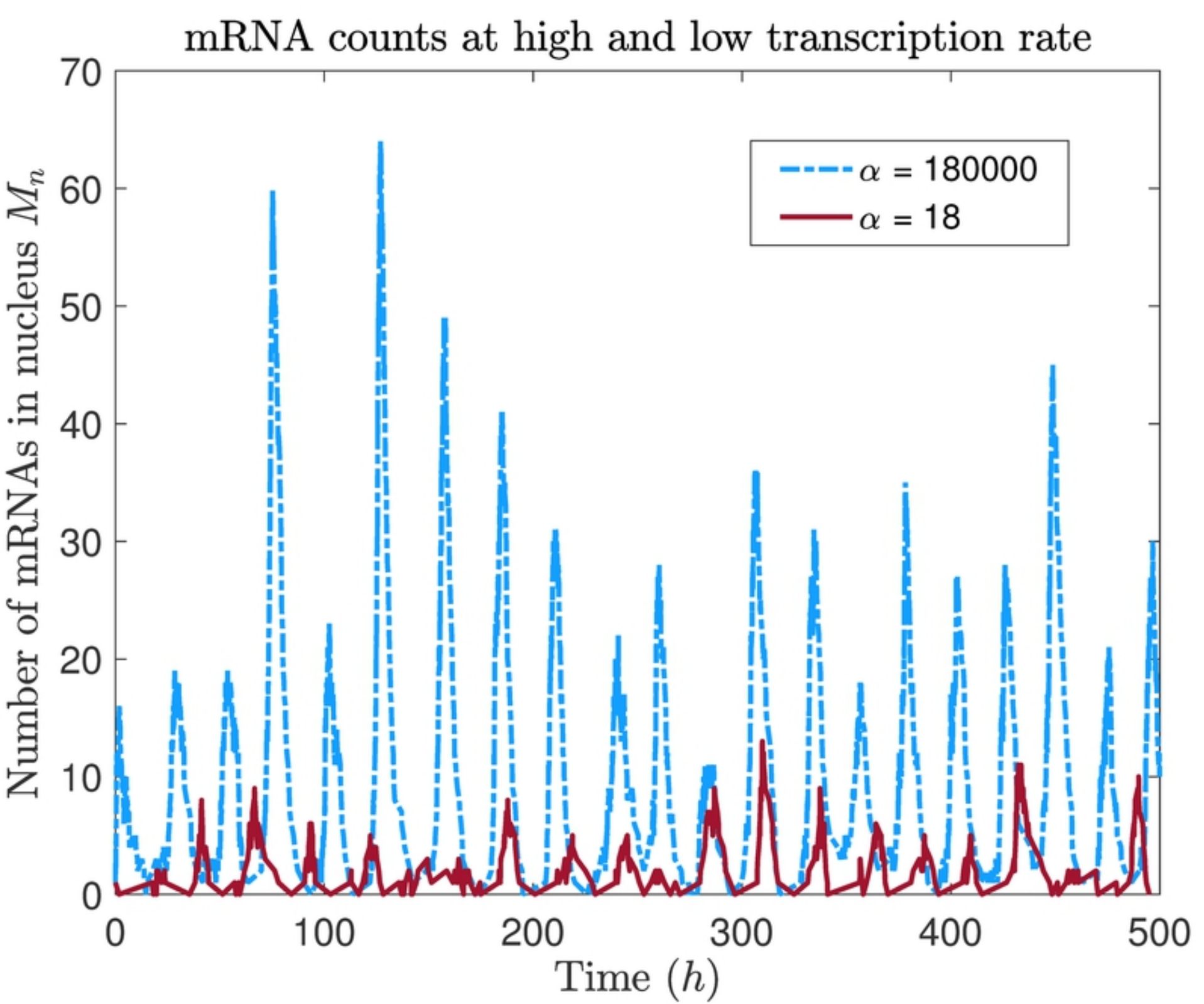
mRNA counts at high and low transcription rate
Number of mRNAs in nucleus M_n
Time (h)
α = 180000
α = 18
0
10
20
30
40
50
60
70
0
100
200
300
400
500

Figure

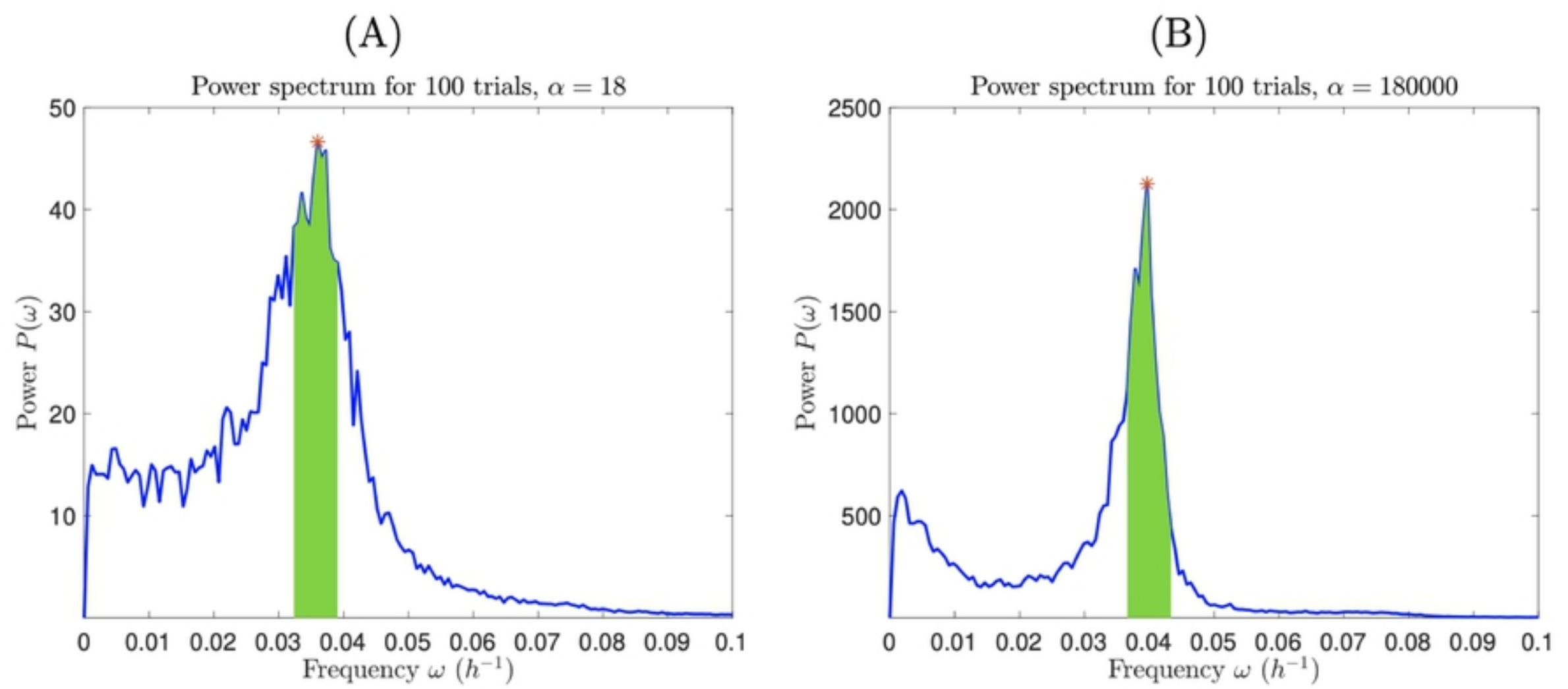
(A)
Power spectrum for 100 trials, $\alpha = 18$
Power $P(\omega)$
Frequency ω (h^{-1})
(B)
Power spectrum for 100 trials, $\alpha = 180000$
Power $P(\omega)$
Frequency ω (h^{-1})

Figure

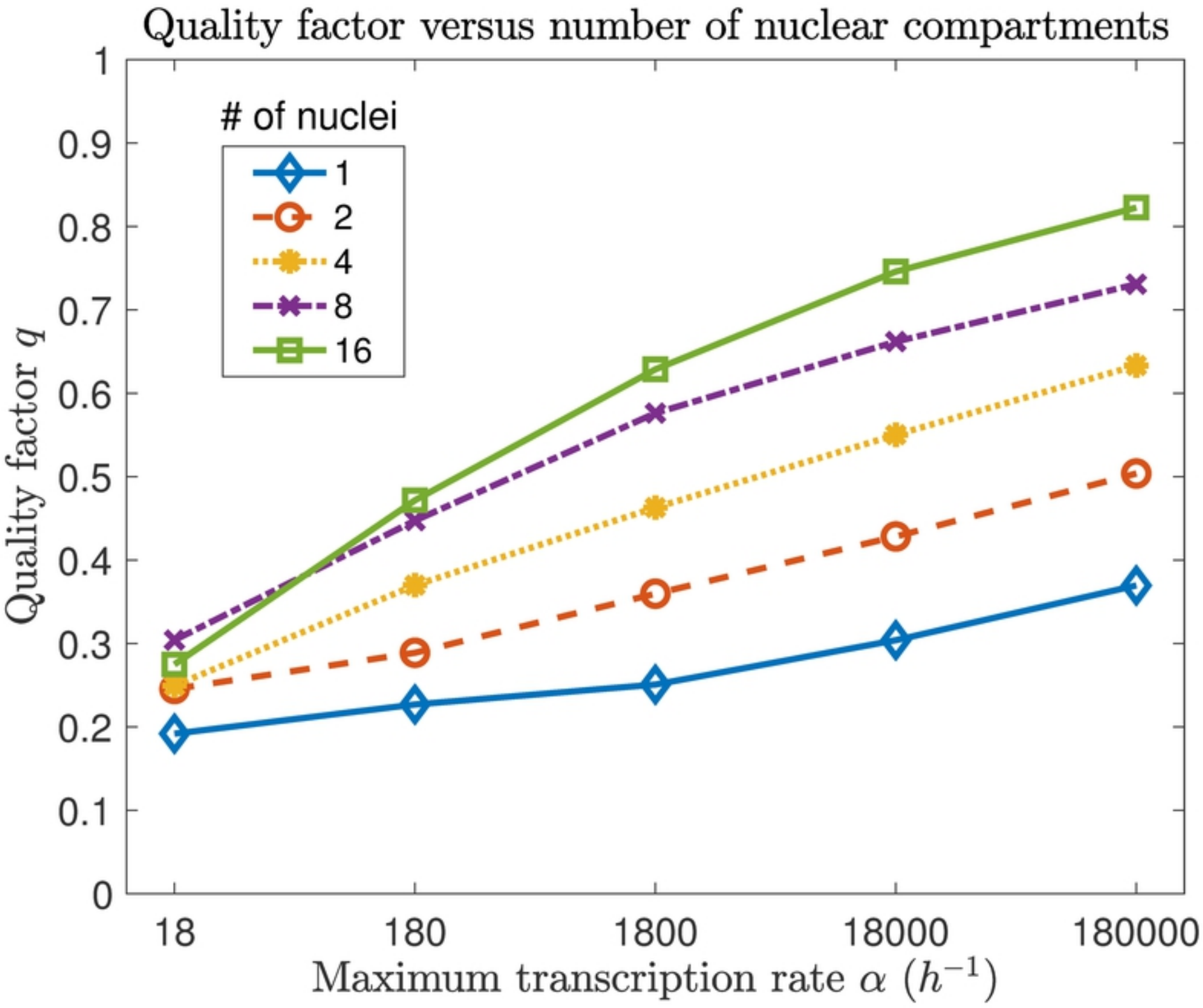
Quality factor versus number of nuclear compartments
# of nuclei
1
2
4
8
16
Quality factor q
0
0.1
0.2
0.3
0.4
0.5
0.6
0.7
0.8
0.9
1
18
180
1800
18000
180000
Maximum transcription rate α (h^{-1})

Figure

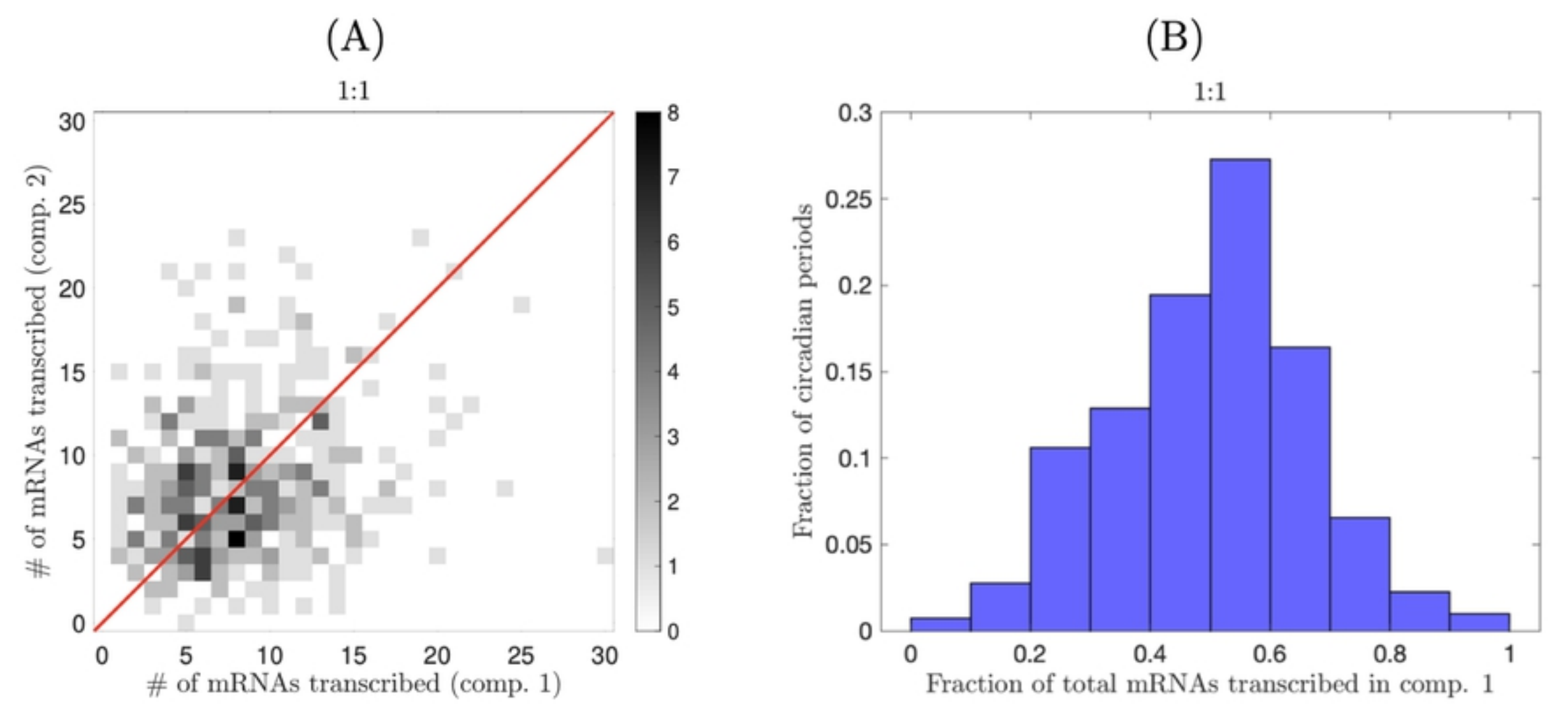
(A)
1:1
# of mRNAs transcribed (comp. 2)
# of mRNAs transcribed (comp. 1)
0
5
10
15
20
25
30
0
1
2
3
4
5
6
7
8
(B)
1:1
Fraction of circadian periods
Fraction of total mRNAs transcribed in comp. 1
0
0.05
0.1
0.15
0.2
0.25
0.3
0.2
0.4
0.6
0.8
1

Figure

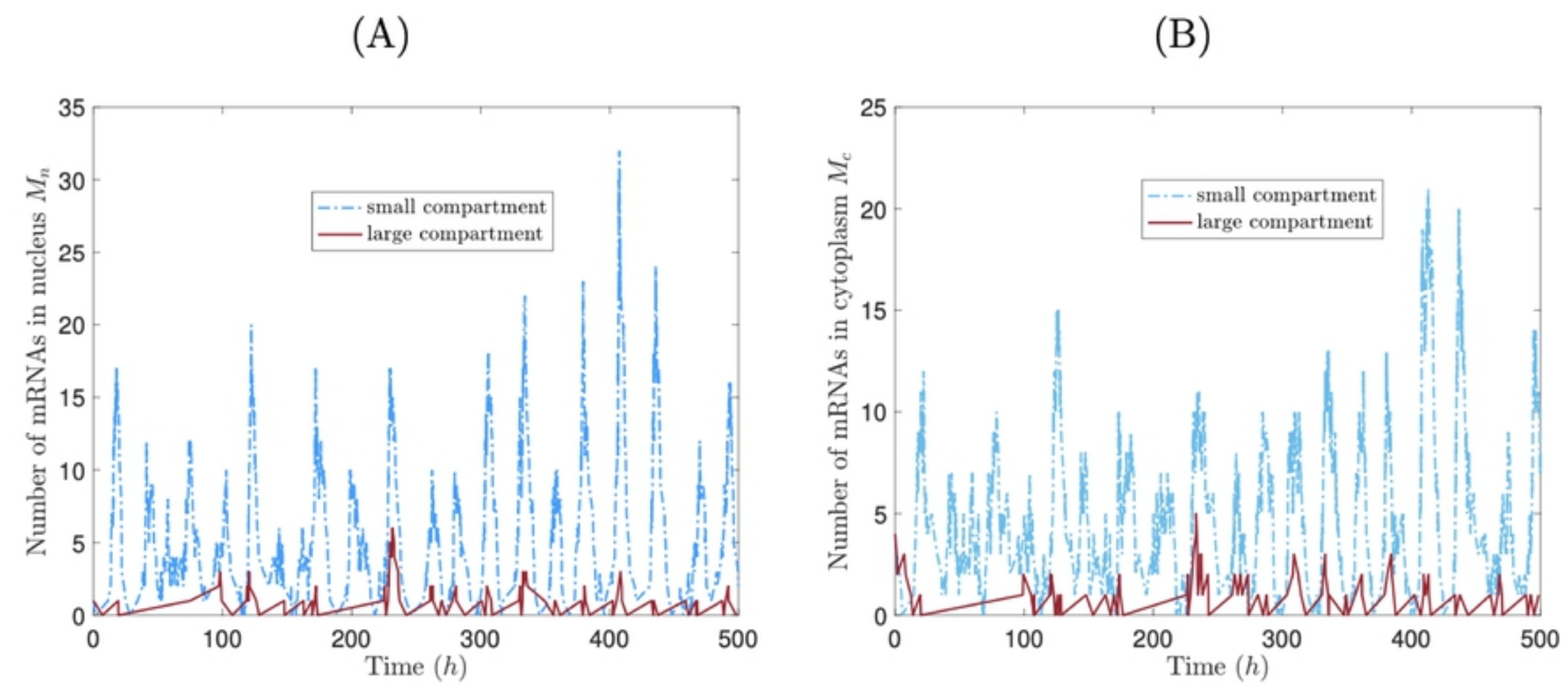
(A)
(B)
small compartment
large compartment
Number of mRNAs in nucleus M_n
Number of mRNAs in cytoplasm M_c
Time (h)
0
5
10
15
20
25
30
35
100
200
300
400
500

Figure

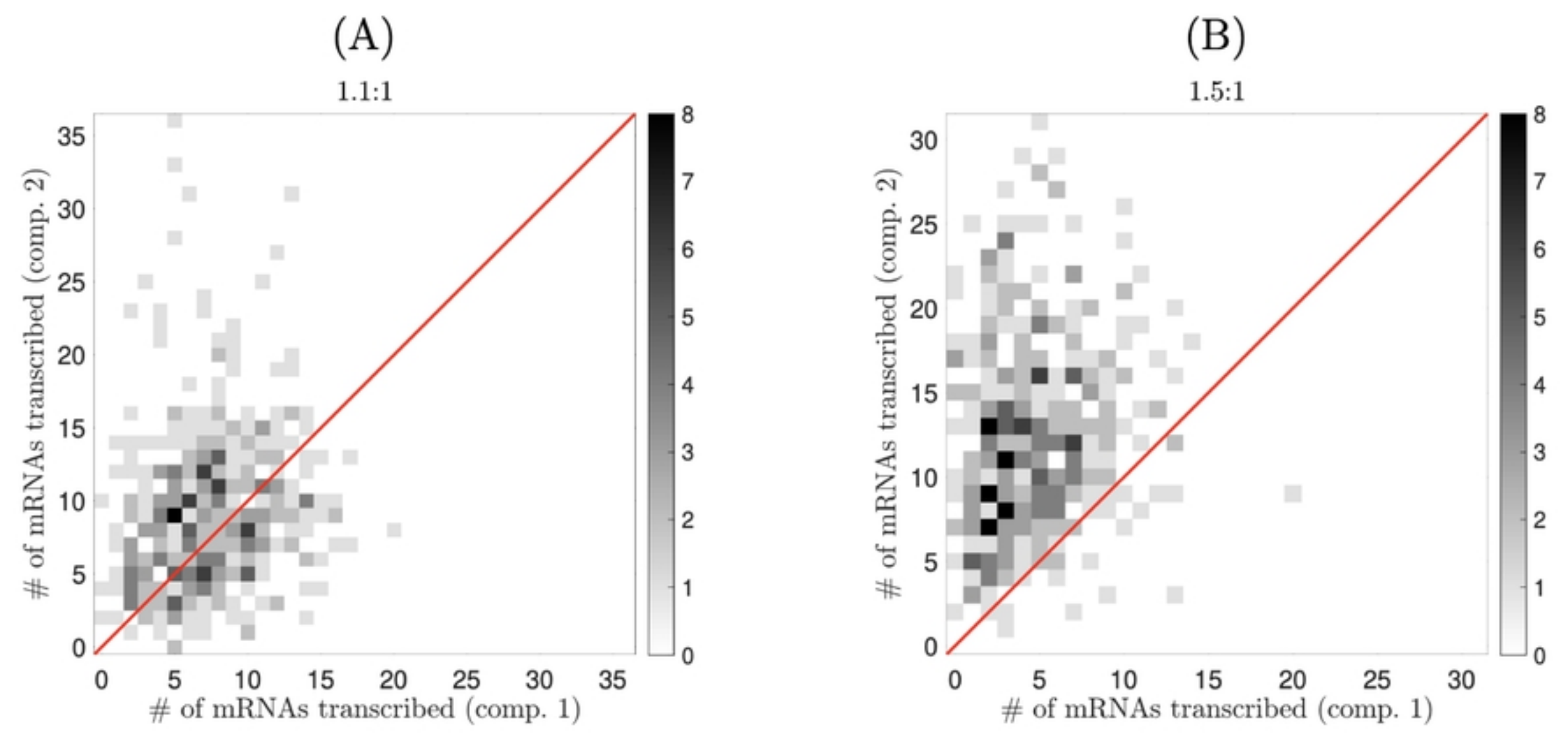
(A)
1.1:1
# of mRNAs transcribed (comp. 2)
# of mRNAs transcribed (comp. 1)
0
5
10
15
20
25
30
35
0
1
2
3
4
5
6
7
8
(B)
1.5:1
# of mRNAs transcribed (comp. 2)
# of mRNAs transcribed (comp. 1)
0
5
10
15
20
25
30
0
1
2
3
4
5
6
7
8

Figure

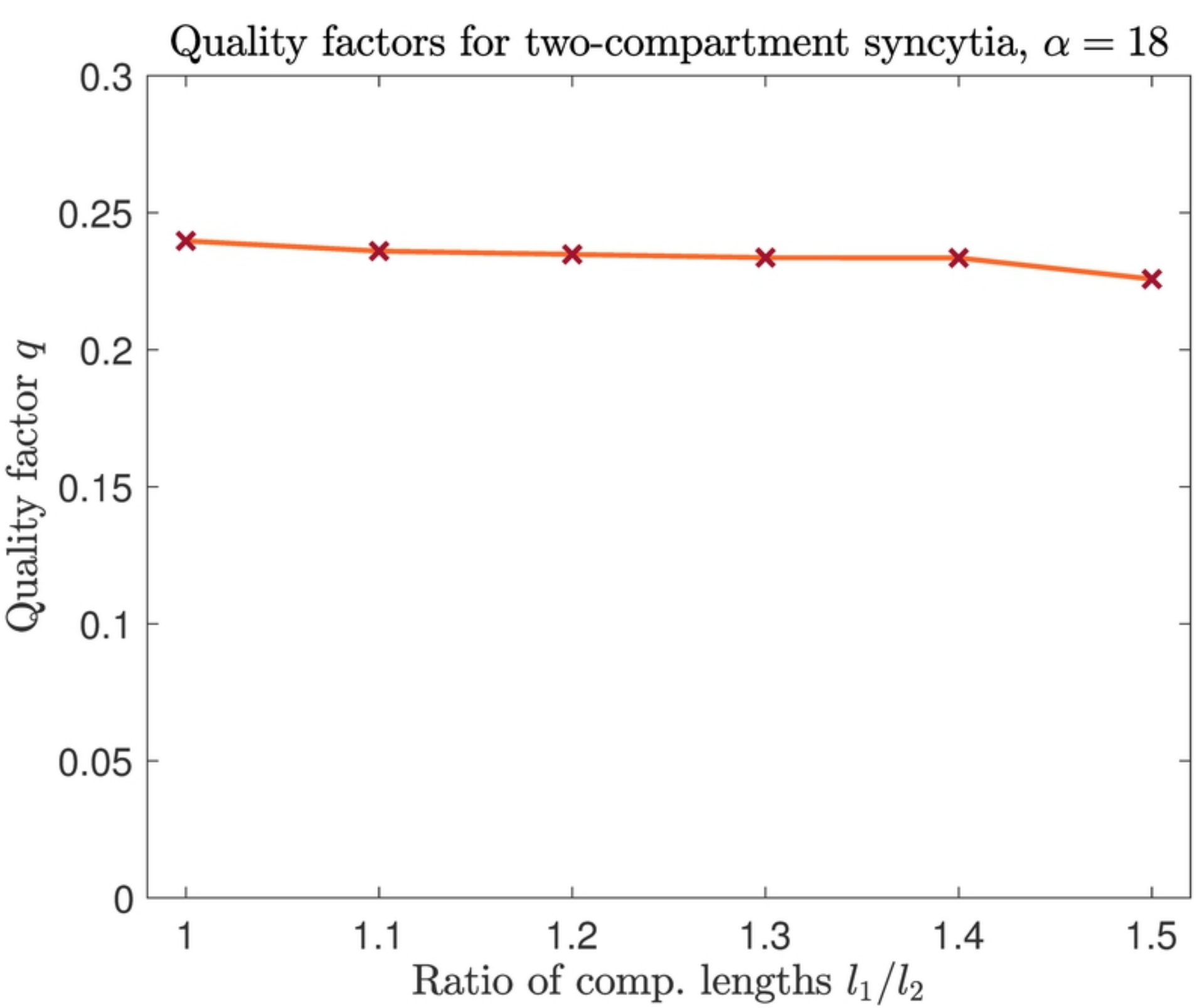
Quality factors for two-compartment syncytia, $\alpha = 18$
Quality factor q
0.3
0.25
0.2
0.15
0.1
0.05
0
1
1.1
1.2
1.3
1.4
1.5
Ratio of comp. lengths l_1/l_2

Figure

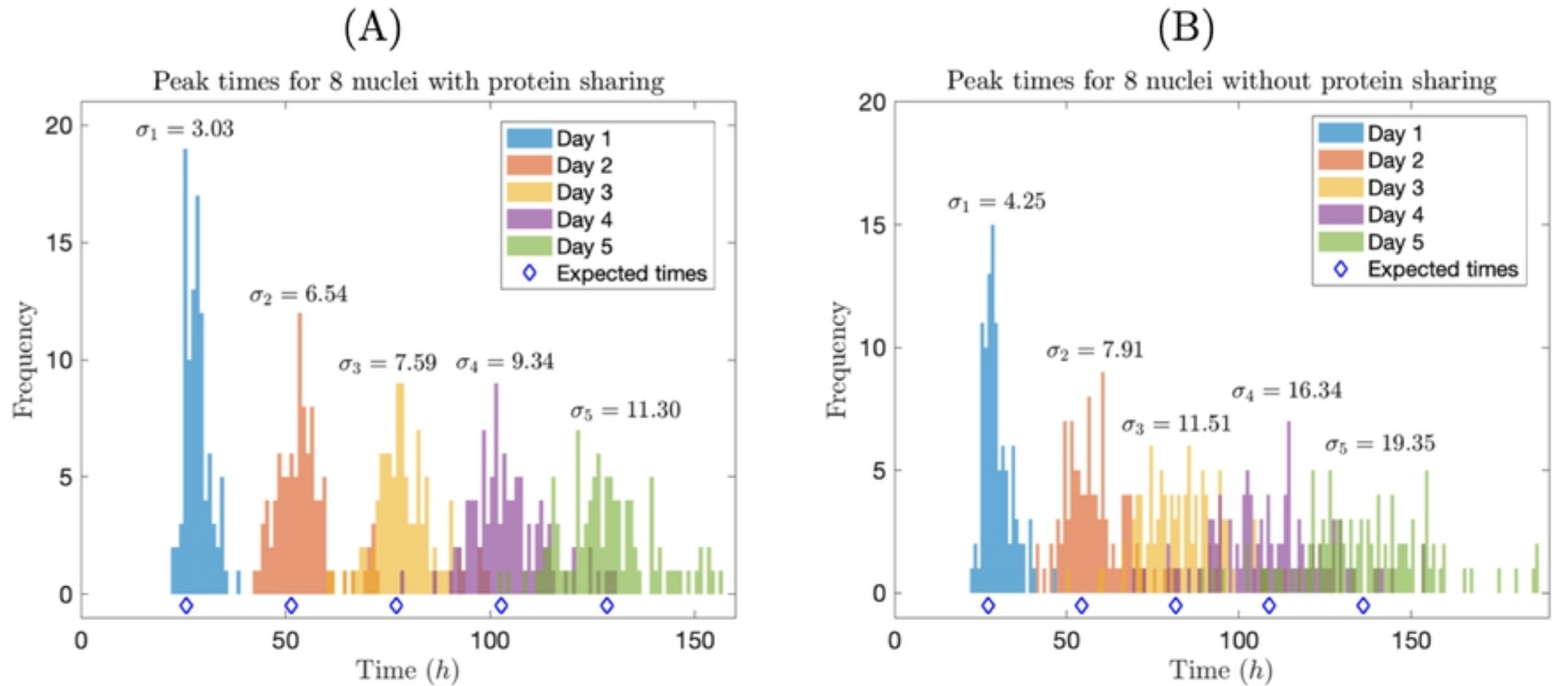
(A)
Peak times for 8 nuclei with protein sharing
$\sigma_1 = 3.03$
$\sigma_2 = 6.54$
$\sigma_3 = 7.59$
$\sigma_4 = 9.34$
$\sigma_5 = 11.30$
Day 1
Day 2
Day 3
Day 4
Day 5
Expected times
Frequency
Time (h)
0
5
10
15
20
0
50
100
150
(B)
Peak times for 8 nuclei without protein sharing
$\sigma_1 = 4.25$
$\sigma_2 = 7.91$
$\sigma_3 = 11.51$
$\sigma_4 = 16.34$
$\sigma_5 = 19.35$
Day 1
Day 2
Day 3
Day 4
Day 5
Expected times
Frequency
Time (h)
0
5
10
15
20
0
50
100
150

Figure